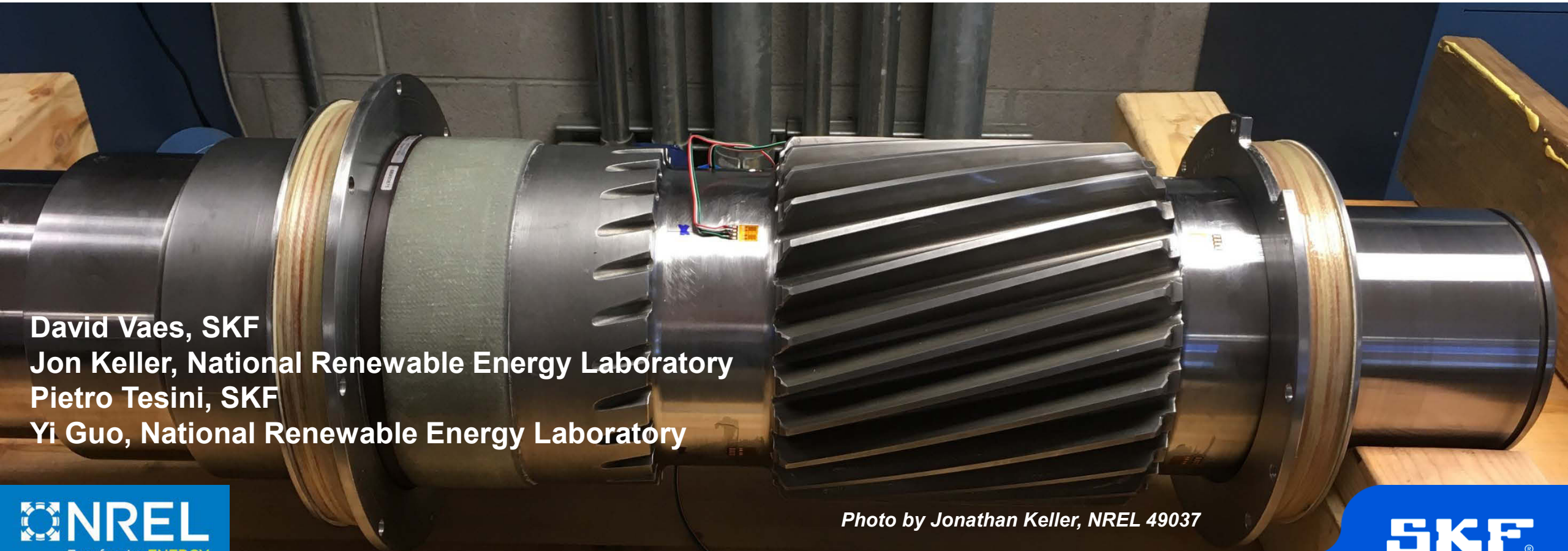


Roller Sliding in Wind Turbine Gearbox High-Speed-Shaft Bearings

4th Conference for Wind Power Drives 2019, Aachen, March 13, 2019

NREL/PR-5000-73428



David Vaes, SKF
Jon Keller, National Renewable Energy Laboratory
Pietro Tesini, SKF
Yi Guo, National Renewable Energy Laboratory

Photo by Jonathan Keller, NREL 49037

Overview

- Background
- Measurement setup
- Numerical model building and verification
- Transient load conditions
- Conclusions

The background of the slide is a high-resolution, close-up photograph of a dark asphalt surface. The surface is heavily textured and shows significant signs of wear and aging, with numerous fine, irregular cracks and larger, more prominent fissures that create a complex, web-like pattern across the frame. The lighting is somewhat uneven, highlighting the rough edges of the cracks and the granular texture of the asphalt.

Background

Photo from SKF

Background: Premature Failures with White Etching Cracks

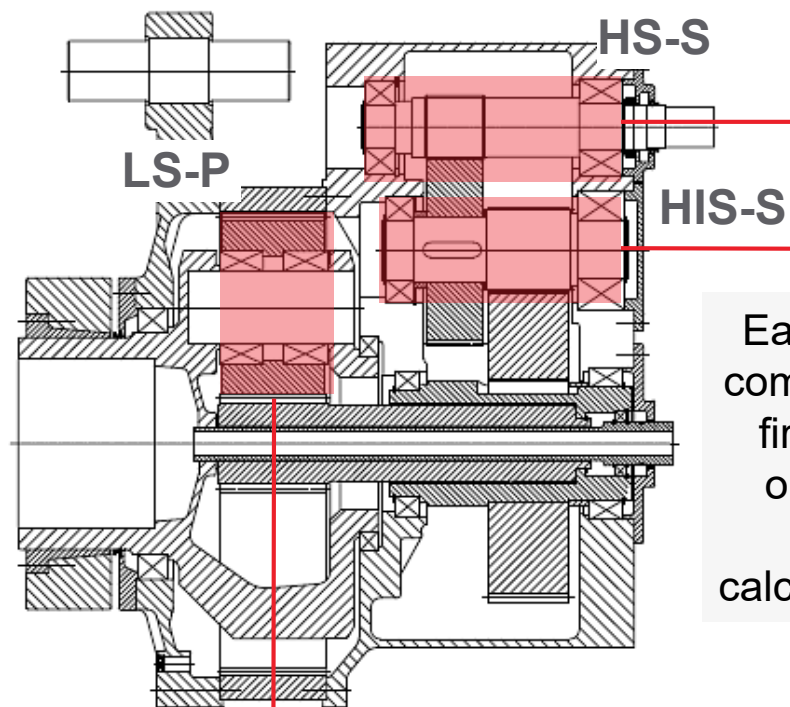
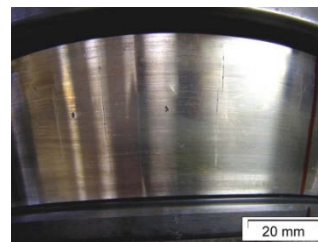
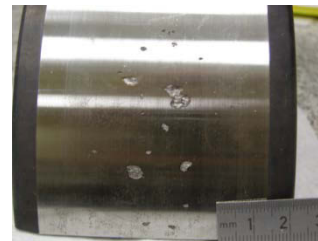


Illustration from SKF

Early cracks occur commonly within the first 1–3 years of operational time (<10% of the calculated rating life).



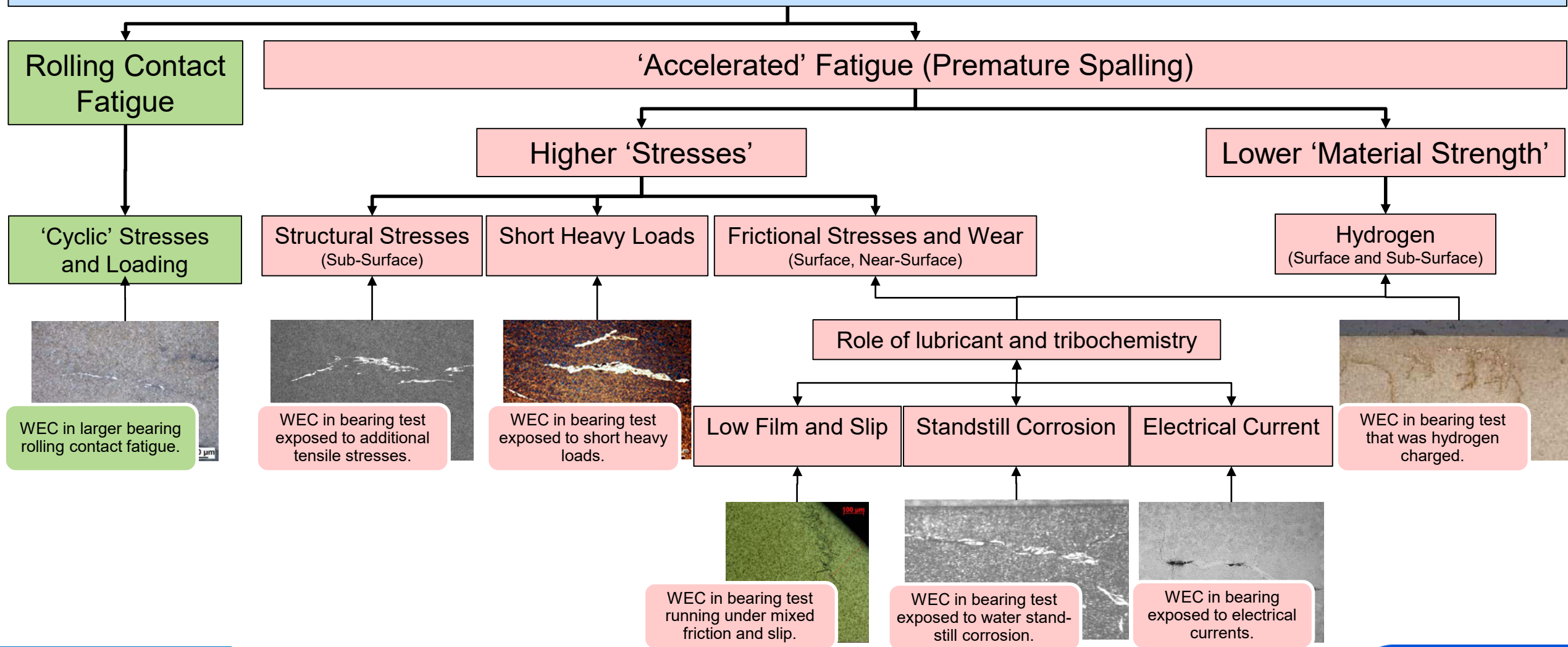
- During recent years several countermeasures have been taken
- Since introduction of black-oxidising, no serial failure case reported by gearbox original equipment manufacturer
- Some failures still reported today by after market and end users:
 - Proper statistics are missing.



Photos from SKF

Premature Bearing Failures: Understanding the Drivers

White Etching Cracks (WECs) Occurrence in Bearings



Photos from SKF

Critical Operating Conditions in Wind Gearboxes

- The exact combination of drivers that explains the failures in wind gear units is not yet understood:
 - Limits of current solutions are not fully understood
 - A better understanding of critical operating conditions in wind gearboxes still required
- Simulations and measurements complete each other.

Simulation

- Requires a detailed set of boundary conditions
- Requires tuning of model parameters
- Disturbances are negligible
- Possibility of in-depth analysis of roller kinematics.



Measurement

- Provides data in complex operating conditions
- Only requires to process the measured signals
- Limited number of output parameters
- Measurement disturbances and input uncertainties.



Photo from SKF



Illustration from SKF



Illustration from SKF

Measurement Setup



Photo by Jonathan Keller, NREL 49037

Gearbox Instrumentation

Winergy PEAB 4410.4 Gearbox and SKF Cylindrical Roller Bearings

- Instrumentation focused on **high-speed shaft, bearings, and lubricant**:
 - Shaft speed
 - Cage speed
 - Roller speed } **Sliding**
- Shaft torque and bending
- Stray current
- Bearing temperatures
- Air temperature and humidity
- Lubricant temperatures and moisture content
- LogiLube and Poseidon lubricant monitoring and routine oil samples
- SKF iMX8 system.



Photo by Mark McDade, NREL 49050

Turbine and Meteorological (Met) Tower Instrumentation

GE 1.5 SLE turbine:

- Blade flap and edge bending
- Blade pitch angles
- Rotor azimuth and speed
- Main shaft torque and bending
- Active and reactive power
- Nacelle yaw
- Tower bending and torsion
- Wind vane offset

M5 met tower:

- Air temperatures and humidity
- Wind speed and direction

And more...GPS time stamped.



Photo by Dennis Schroeder, NREL 21884

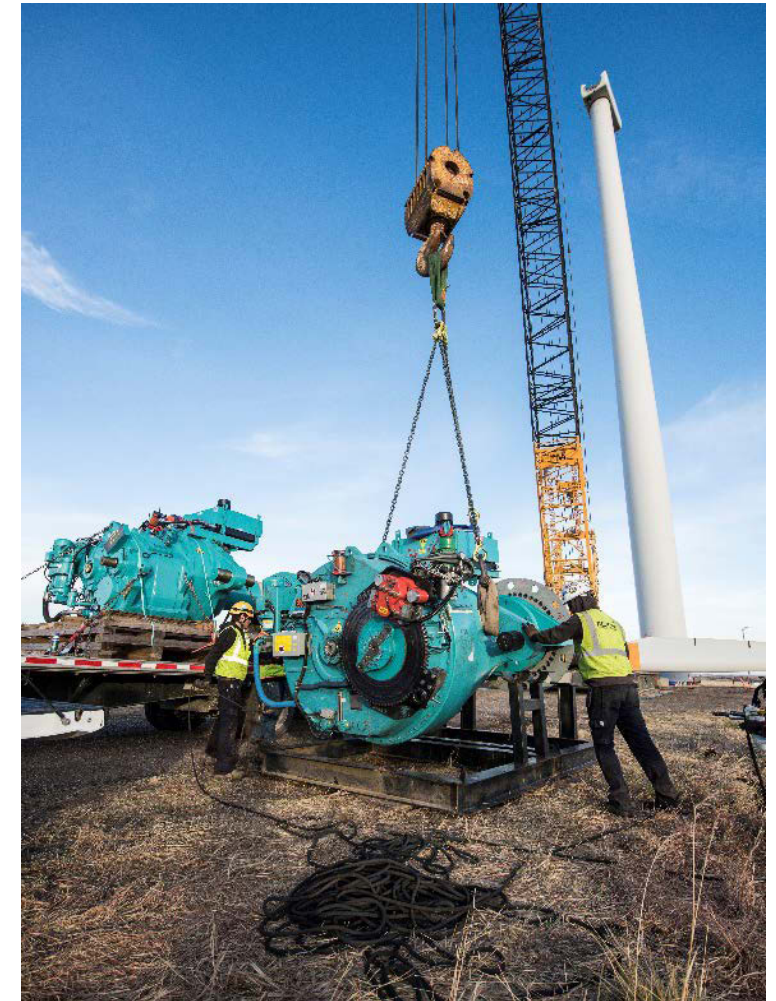
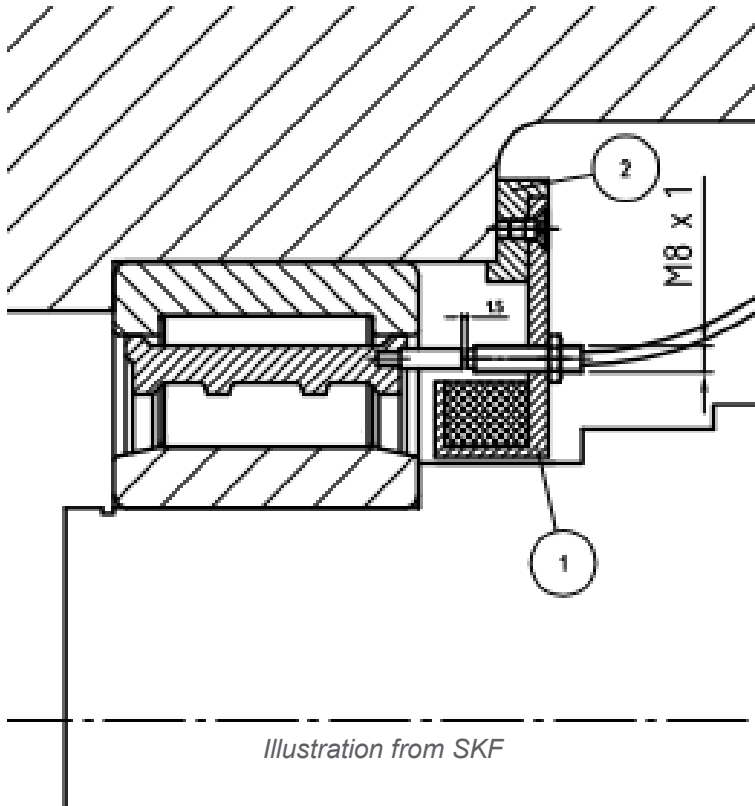


Photo by Dennis Schroeder, NREL 49409

Roller and Cage-Speed Measurement

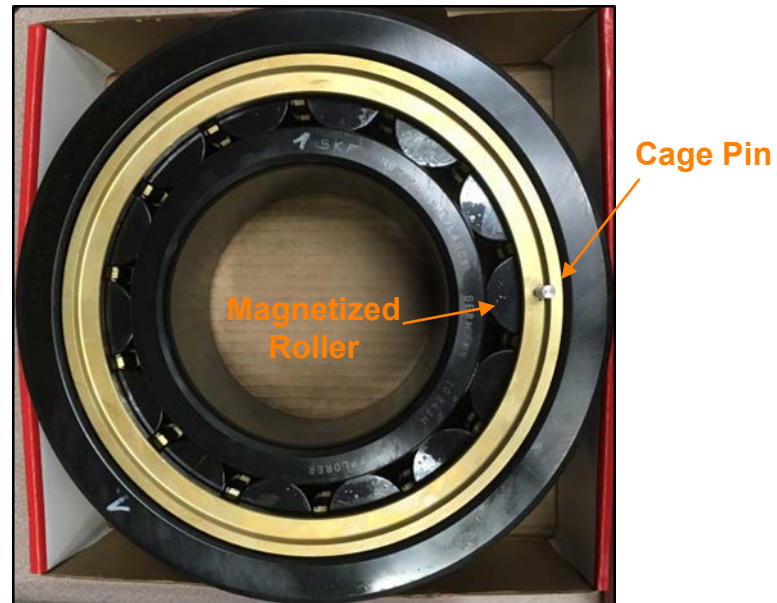


Cage-speed measurement:

- Pin passage detected by proximity sensor
- One speed measurement per cage revolution.

Roller-speed measurement:

- Magnetized roller
- Changing magnetic field detected by coil next to the bearing
- Position of magnetized roller determined by cage pin.



Photos by Jonathan Keller, NREL 40979 and 40981

Numerical Model Building and Verification

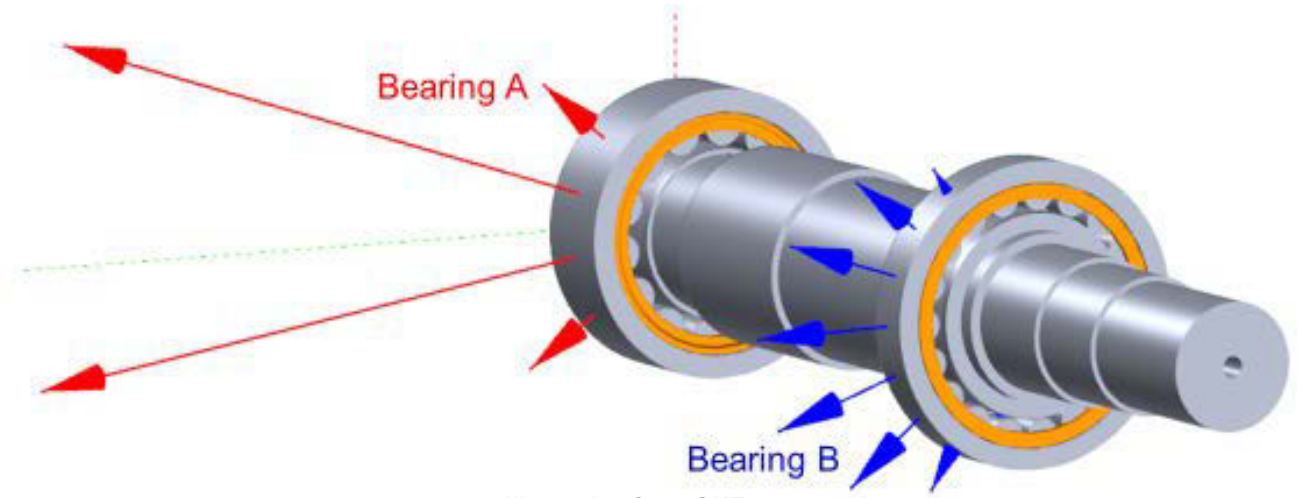


Illustration from SKF

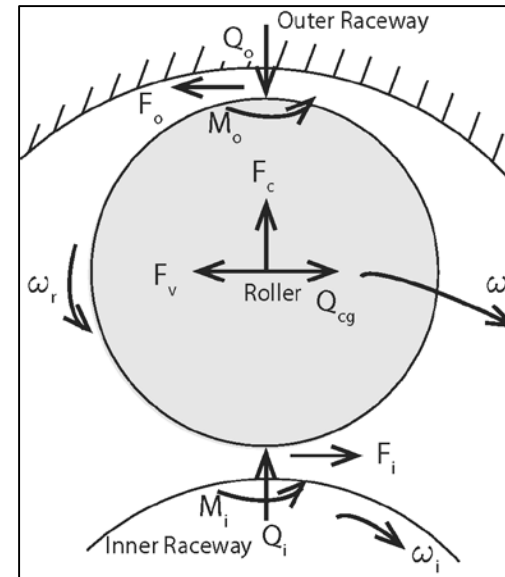


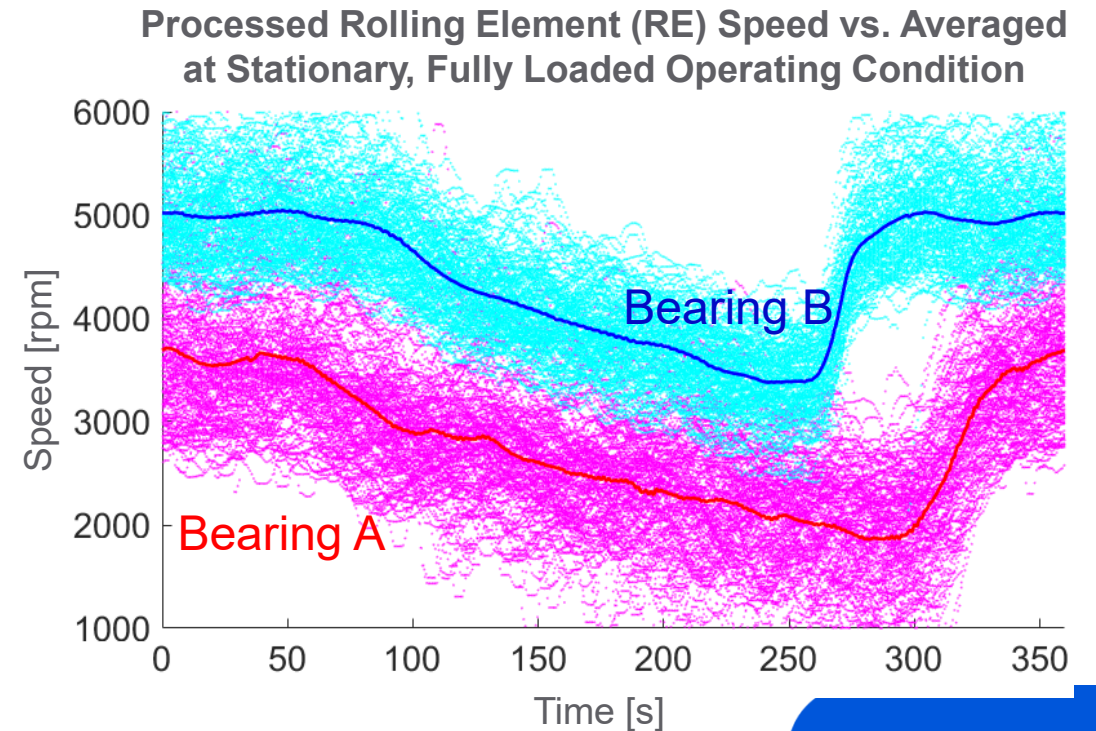
Illustration by NREL

Measurement Limitations and Processing

- Mean cage speed during each revolution is available
- Instantaneous roller speed is available but highly disturbed
- Operating bearing clearance is unknown (bearing inner ring temperature often not available)

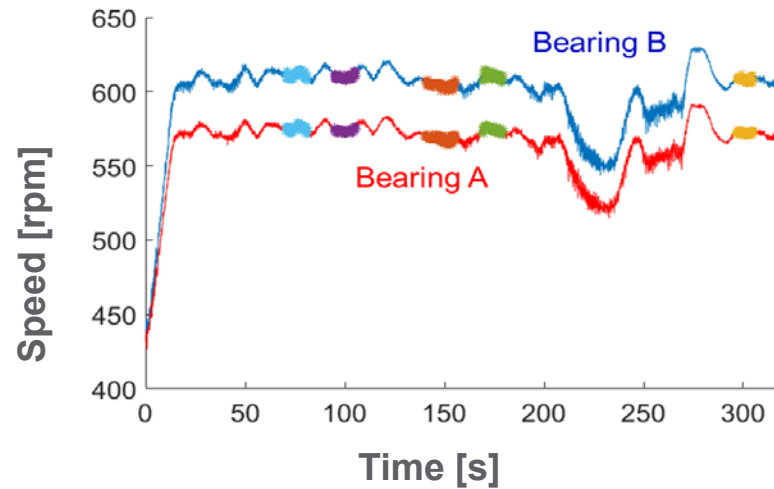
Postprocessing of the measurement is necessary:

1. Select time intervals where the cage speed is constant
2. Use several cage revolutions to filter the disturbance of the roller speed
3. Select best measured intervals.

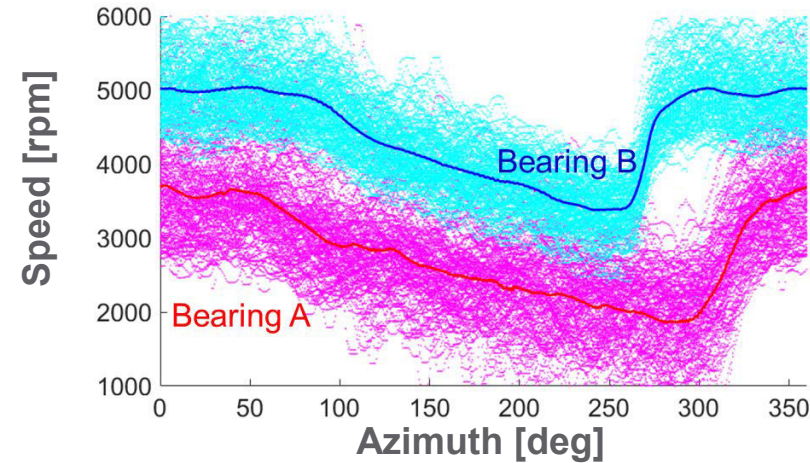


Measurement Screening

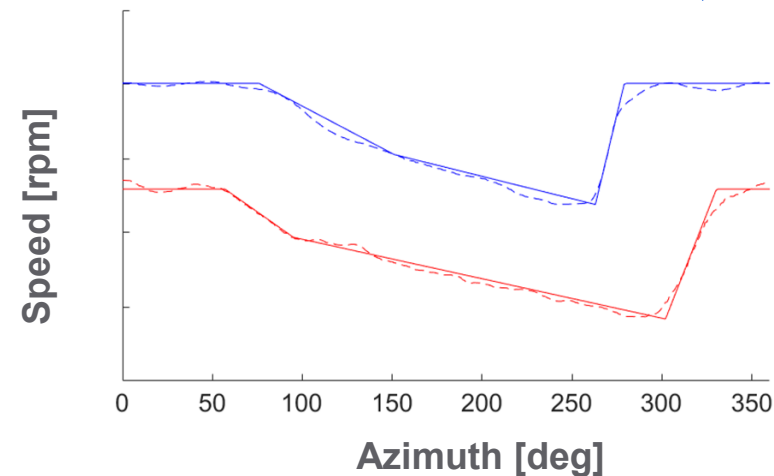
1. Systematic detection of all cage-speed plateaus:



2. Least-squares fit of a piece-wise approximation of the roller speed:



3. Systematic selection based on error:

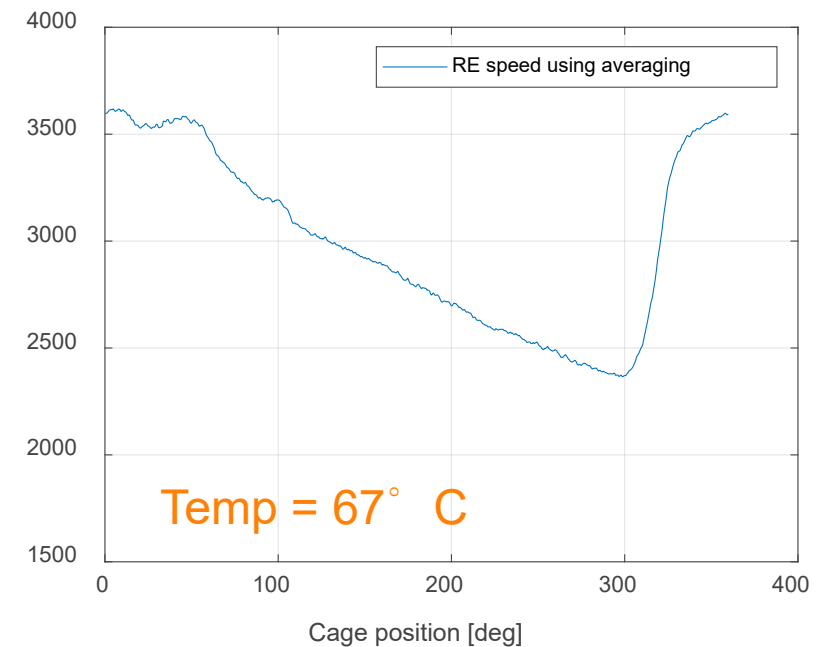
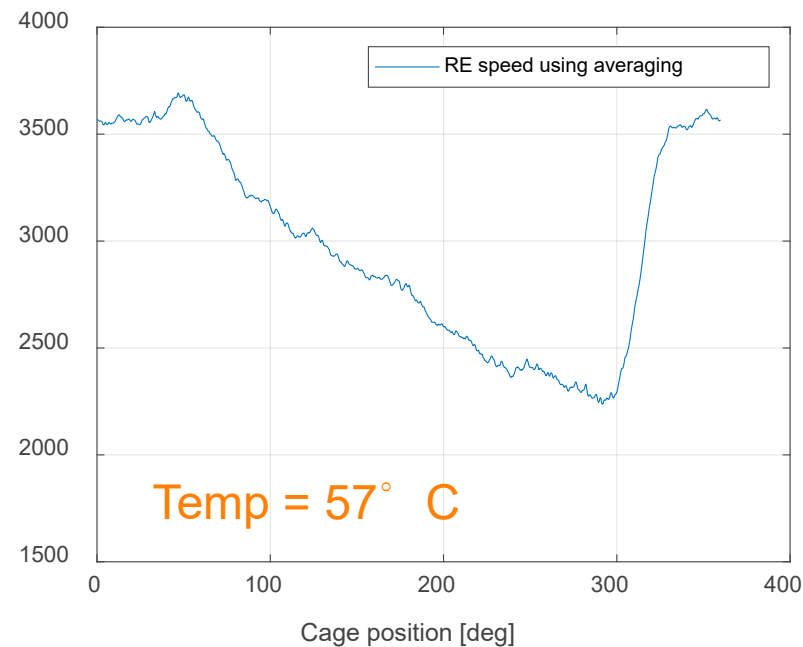
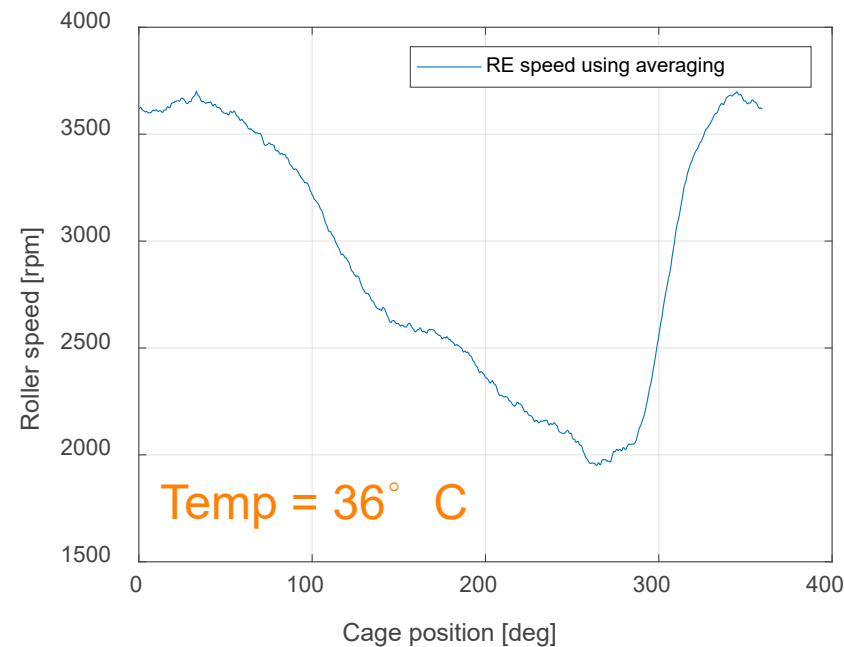


Final selection, based on most interesting and diverse operating conditions to increase the validity of the semiempirical model.

rpm = revolutions per minute | s = seconds | deg = degree

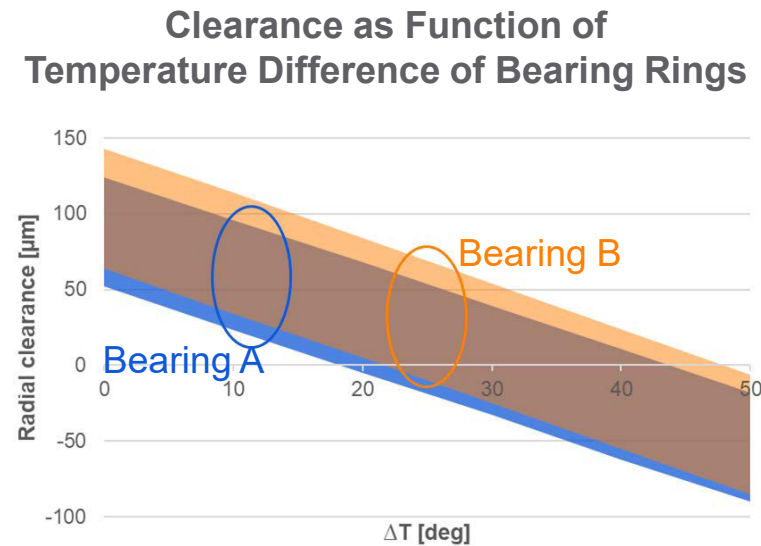
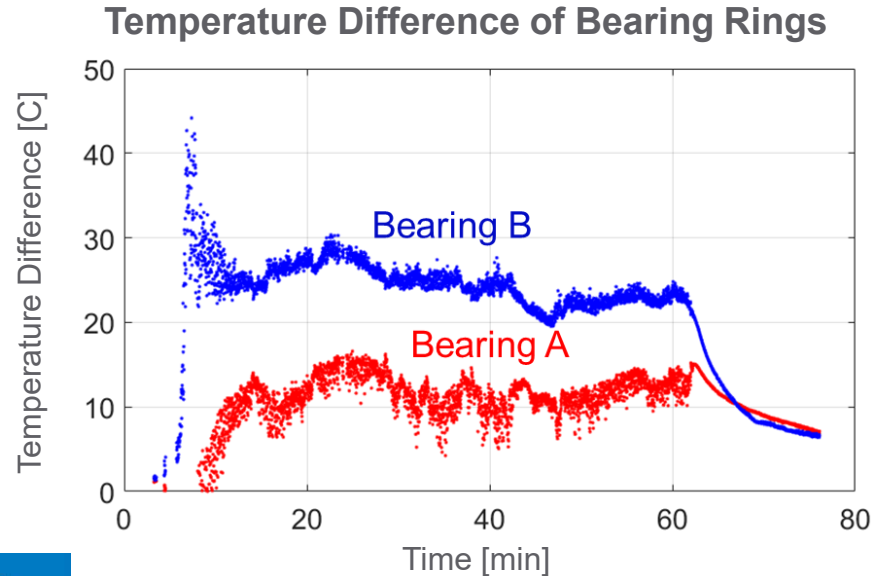
Effect of Temperature on Roller Speed: “Down Slope”

- At lower operating temperature, the rollers decelerate significantly more in unloaded zone
- Higher temperature → lower viscosity → less drag losses on rollers in unloaded zone → slower deceleration



Effect of Temperature and Oil Viscosity – Overview

- A significantly larger temperature difference is measured on bearing B than on bearing A:
 - Bearing B has much smaller radial clearance and a larger loaded zone than bearing A
- Slower deceleration of the rollers in unloaded zone at increasing temperature (lower oil viscosity)
- Drag losses increase with the size of the roller (larger projected surface of the rollers).

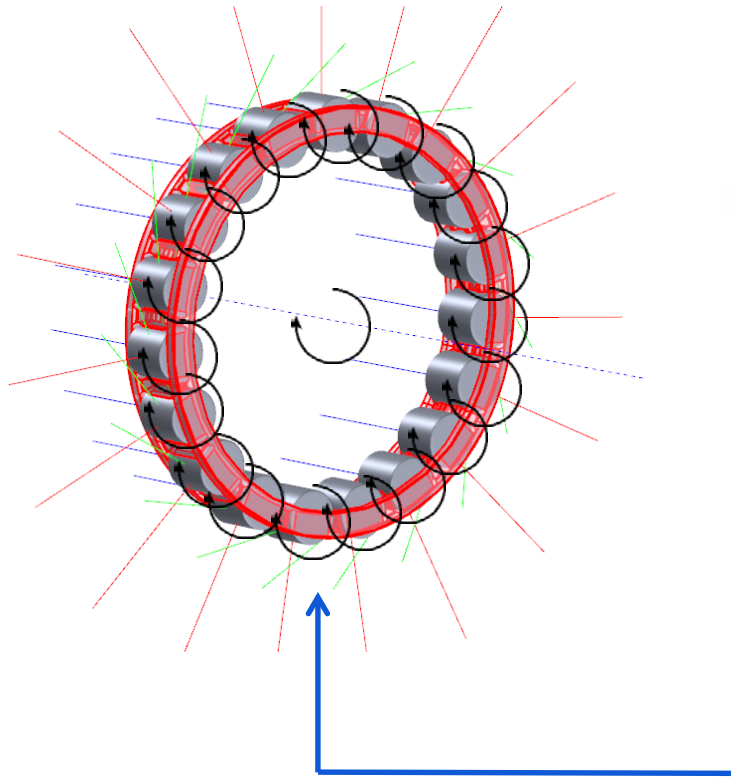


min = minute | μm = micrometers

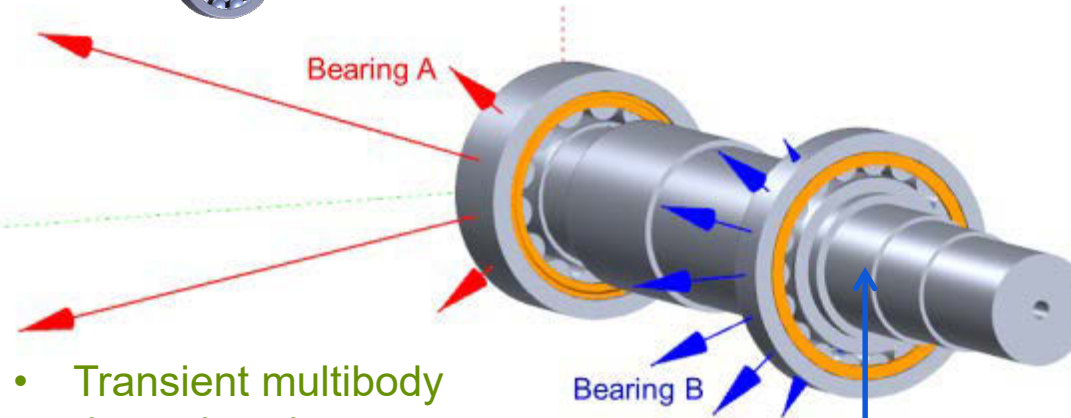
SKF Numerical Modelling

The model is designed by two SKF proprietary software.

Linear rotational damping torque is applied to both the cage and the rollers.

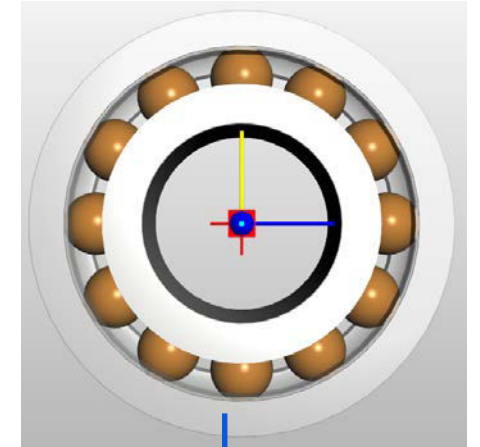


SKF BEAST



- Transient multibody dynamic solver
- Detail contact calculation, elastohydrodynamic layer lubrication
- Cage-roller interaction
- Drag losses not automatically modeled.

SKF SimProExpert



QJ bearing replaced by nonlinear stiffness.

Analytical Model Predicts Roller and Cage Sliding

Roller Free Body Diagram

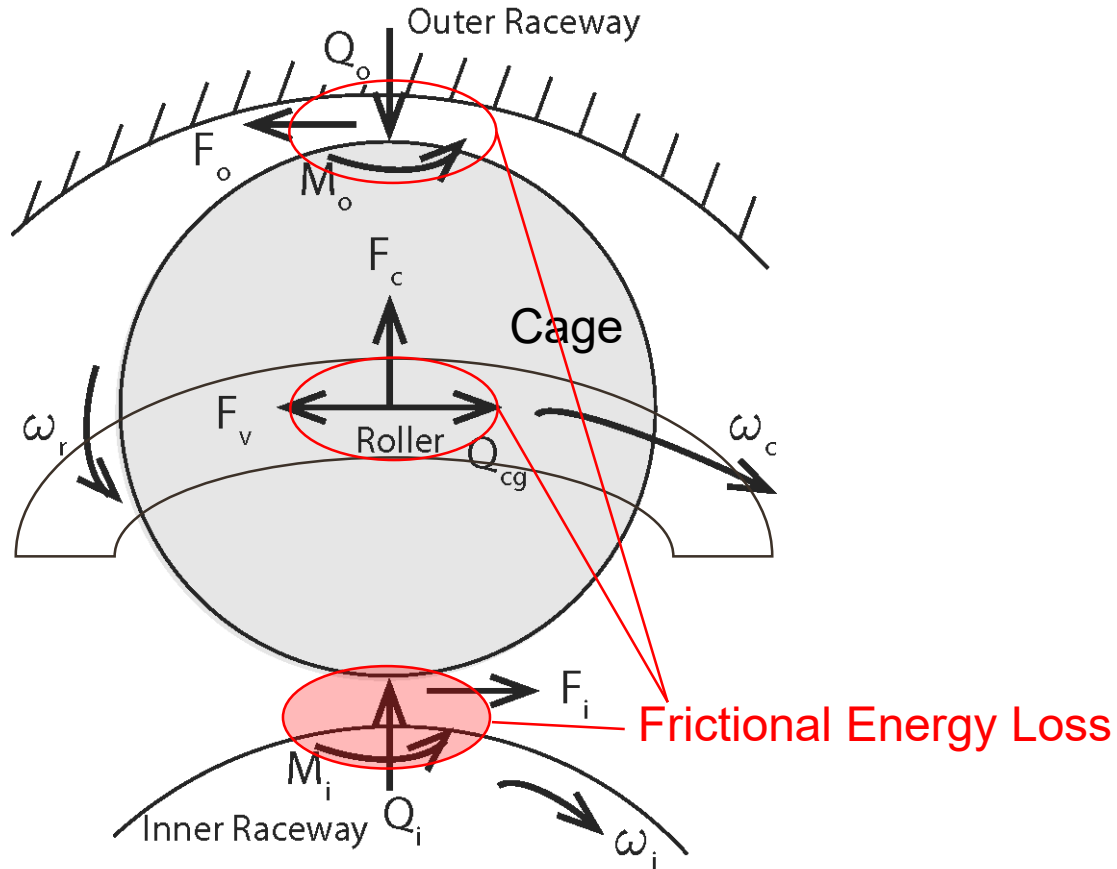


Illustration by NREL

Primary Governing Equations

$$\left\{ \begin{array}{ll} F_{ij} - F_o + F_v - Q_{cg} = 0 & \text{Tangential} \\ Q_i - Q_o + F_c = 0 & \text{Radial} \\ M_i - M_o + \frac{1}{2} \mu_{cg} D Q_{cg} = J \omega_c \frac{d\omega_r}{d\phi} & \text{Torsional} \end{array} \right.$$

Source: Guo, Y. and J. Keller. Forthcoming. Analytic Formulations of Rolling Element Bearing Sliding in Wind Turbine Gearboxes, Mechanism and Machine Theory.

Roller dynamics model (analytical):

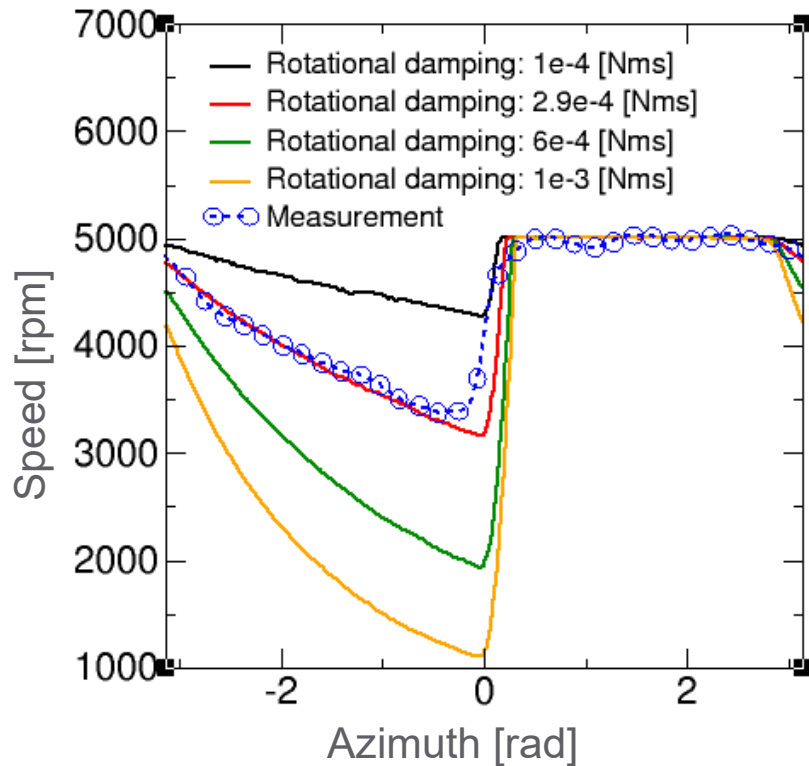
- Harris roller dynamics model

Lubricant hydrodynamics model based on:

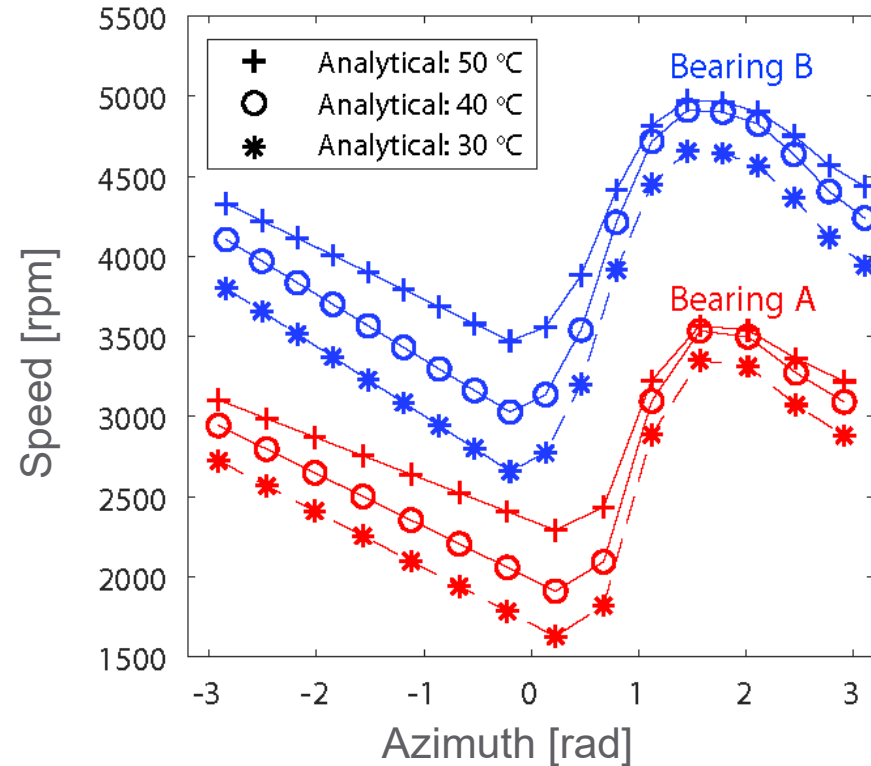
- Bercea cage friction model
- Dowson and Higginson lubricant model

Parametric Studies To Verify Model Parameters

Example in BEAST: Influence of Rotational Damping



Example in Analytical Model: Influence of Temperature



Verification of Simulation Results

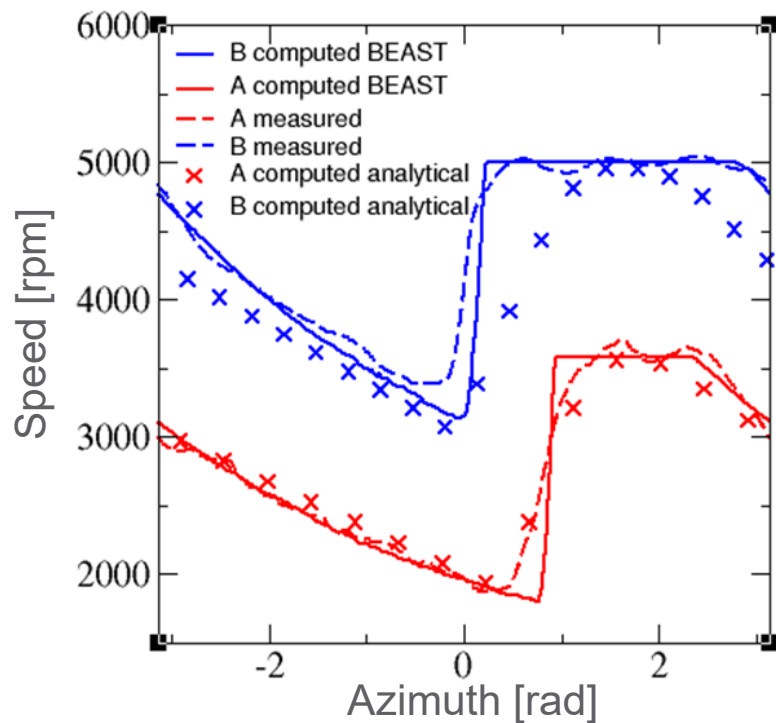
Input

Torque = 7,930 Nm,
 $T_{OR} \sim 41^{\circ}\text{C}$, $T_{oil} = 45^{\circ}\text{C}$
 $\delta_B = 5\mu\text{m}$, $\delta_A = 95\mu\text{m}$

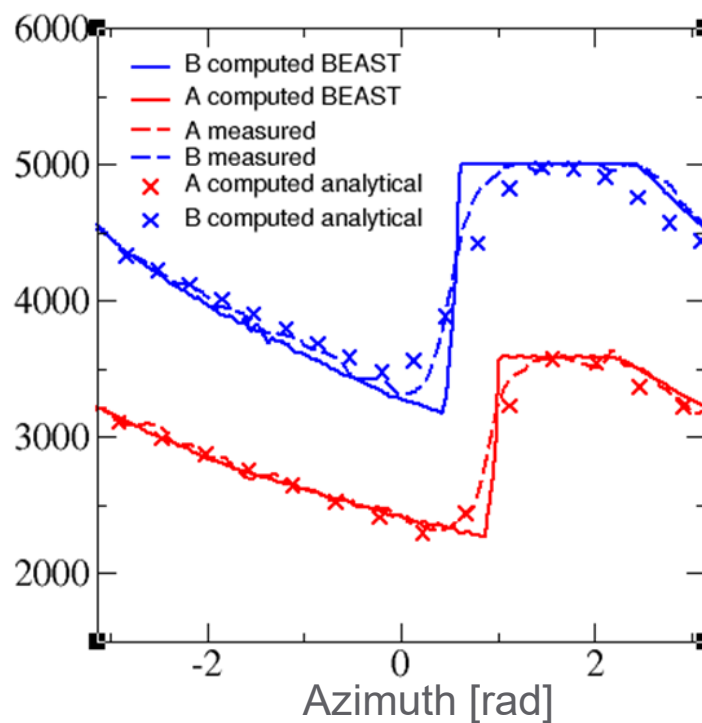
Torque = 7,930 Nm,
 $T_{OR} \sim 63^{\circ}\text{C}$, $T_{oil} = 63^{\circ}\text{C}$
 $\delta_B = 30\mu\text{m}$, $\delta_A = 145\mu\text{m}$

Torque = 9,520 Nm,
 $T_{OR} \sim 57^{\circ}\text{C}$, $T_{oil} = 41^{\circ}\text{C}$
 $\delta_B = 20\mu\text{m}$, $\delta_A = 145\mu\text{m}$

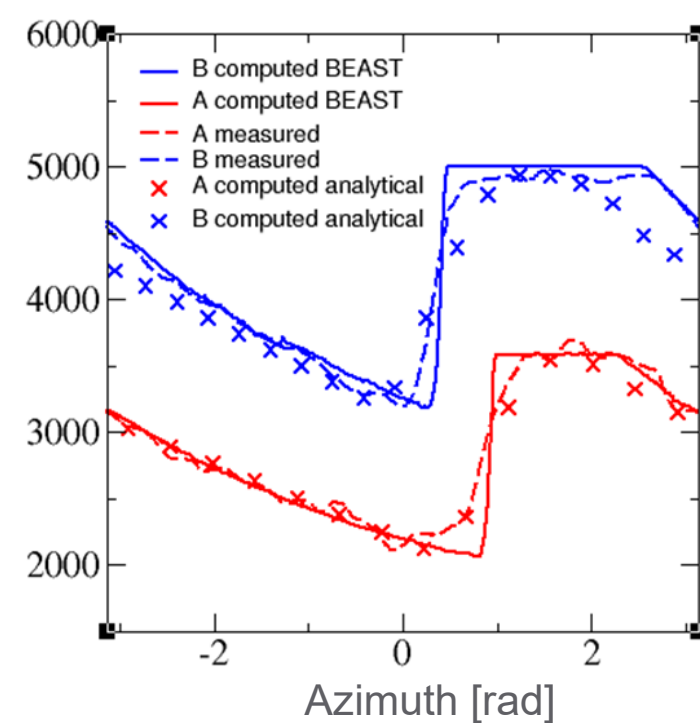
Roller Speeds



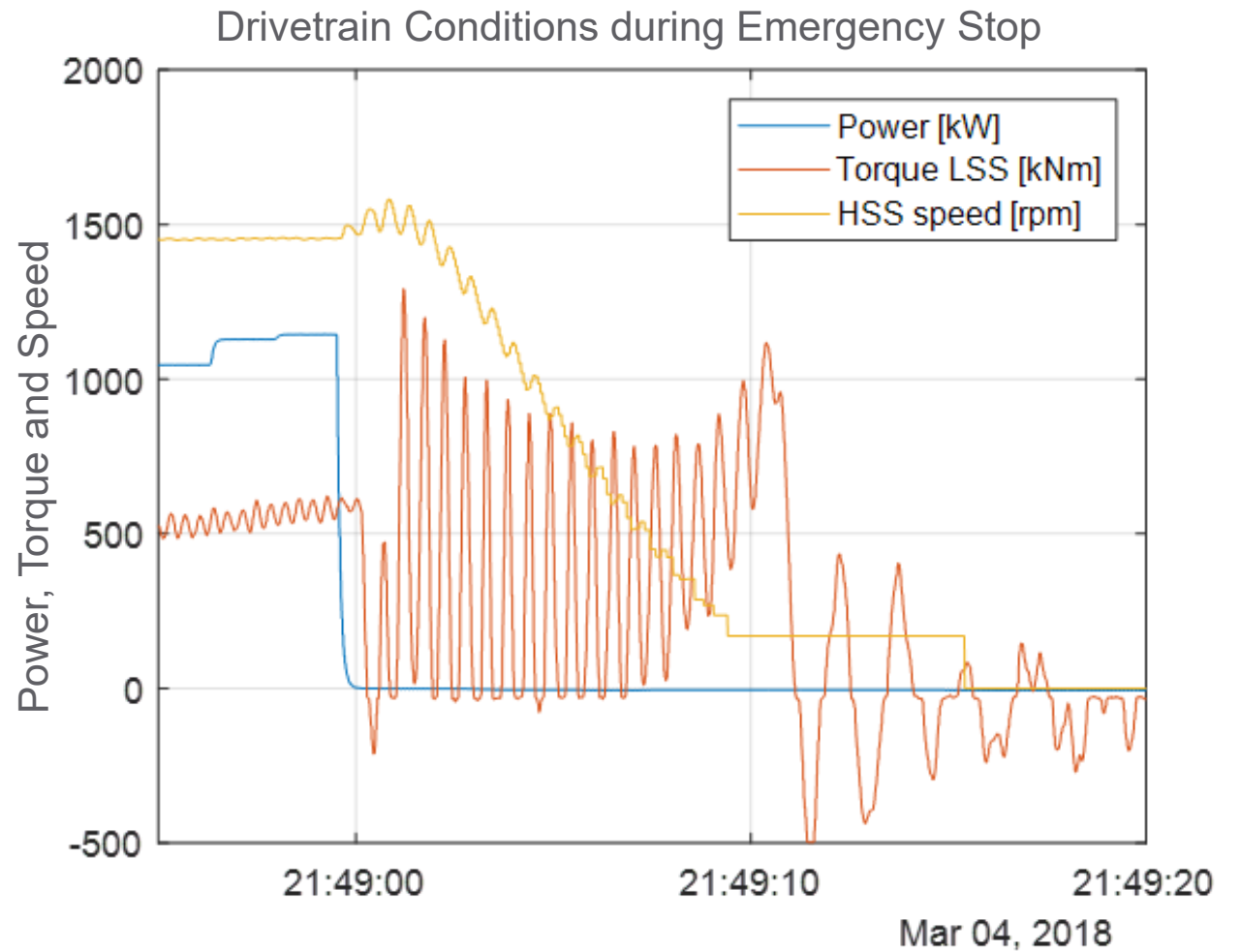
Roller Speeds



Roller Speeds

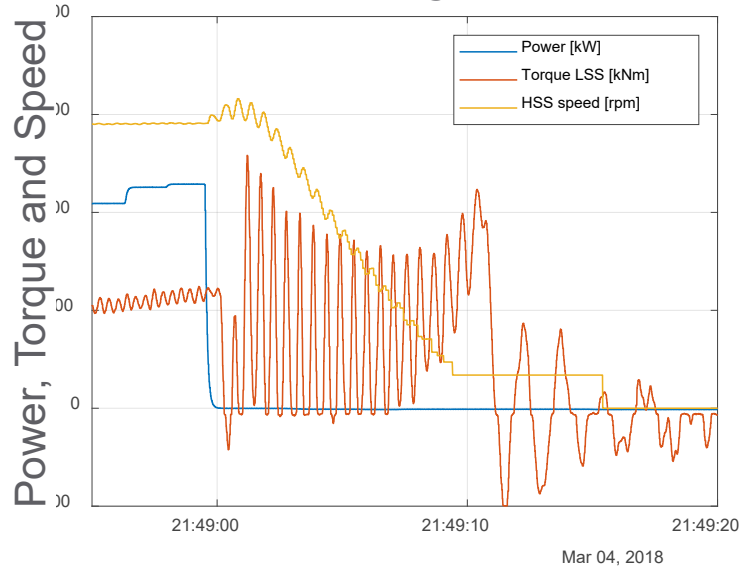


Measurements at Transient Conditions

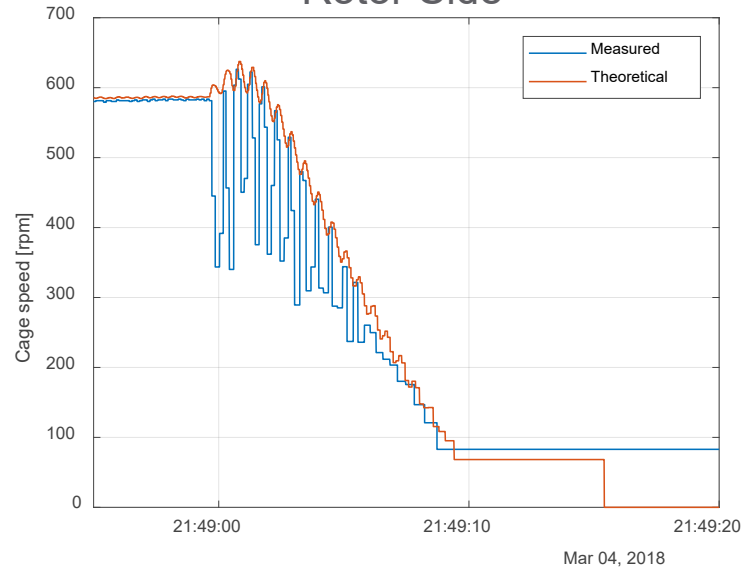


Transient Conditions – Emergency Stop

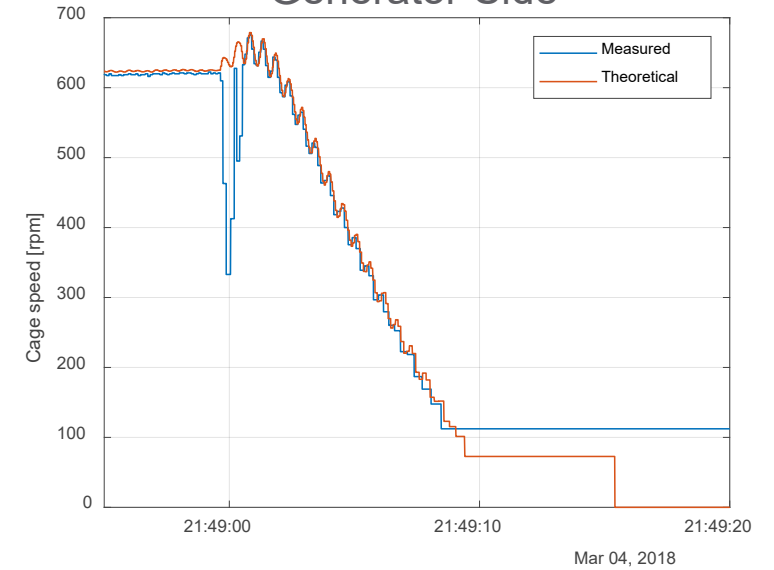
Drivetrain Conditions



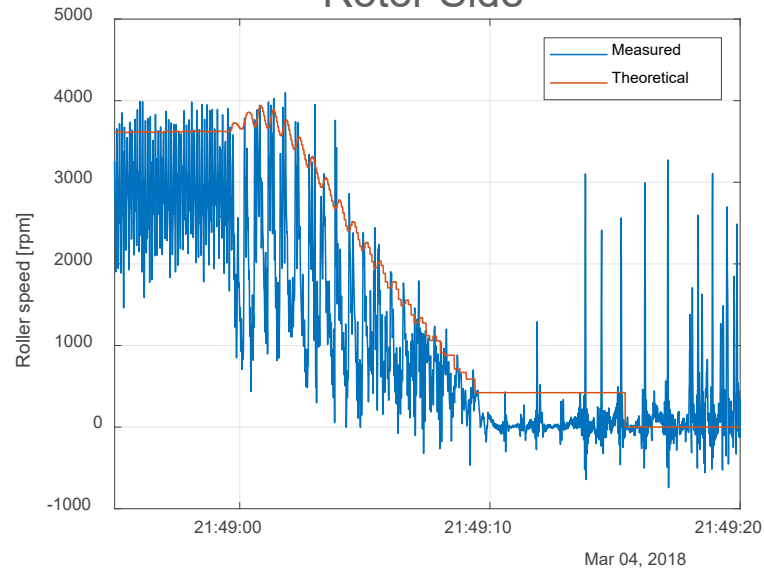
Rotor Side



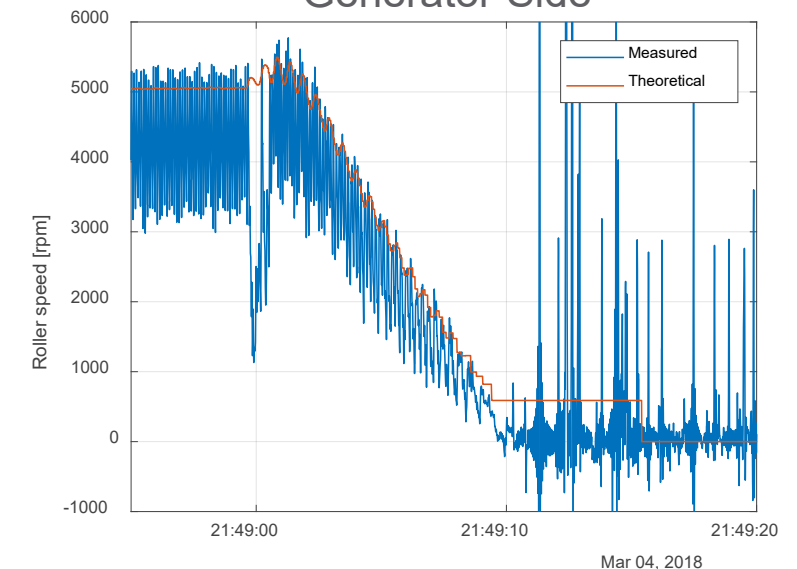
Generator Side



Rotor Side

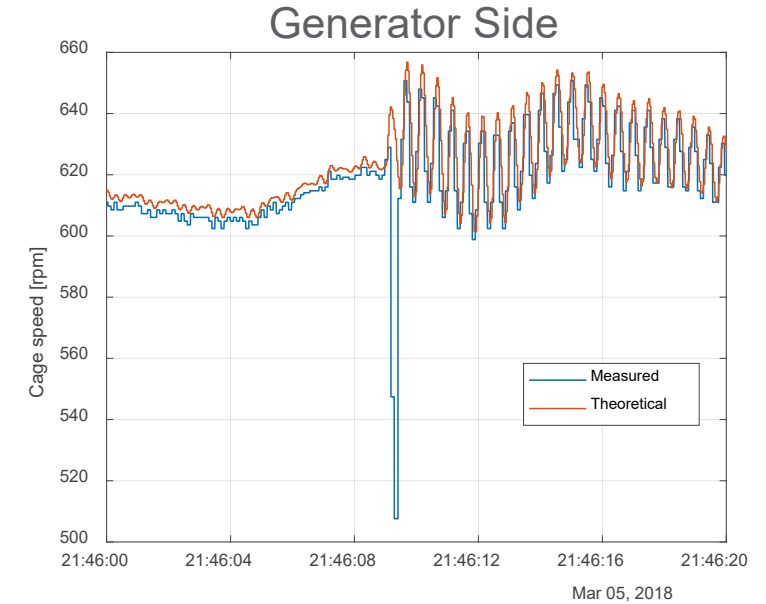
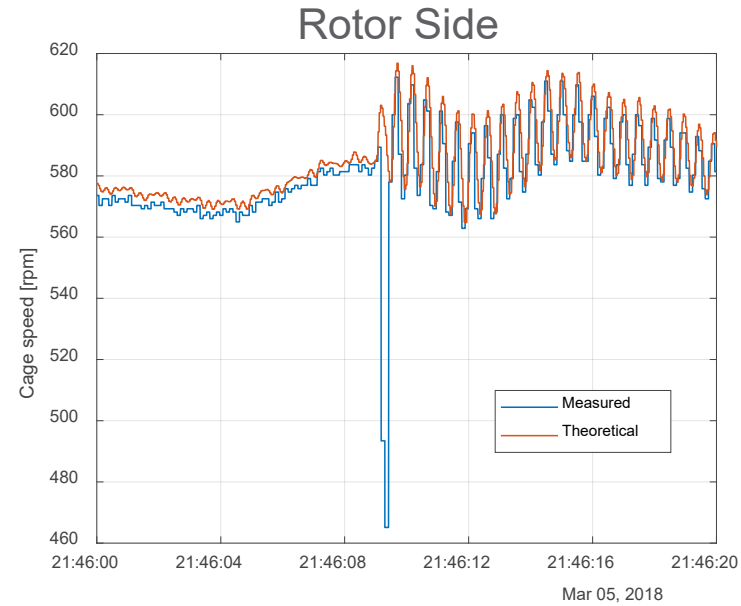
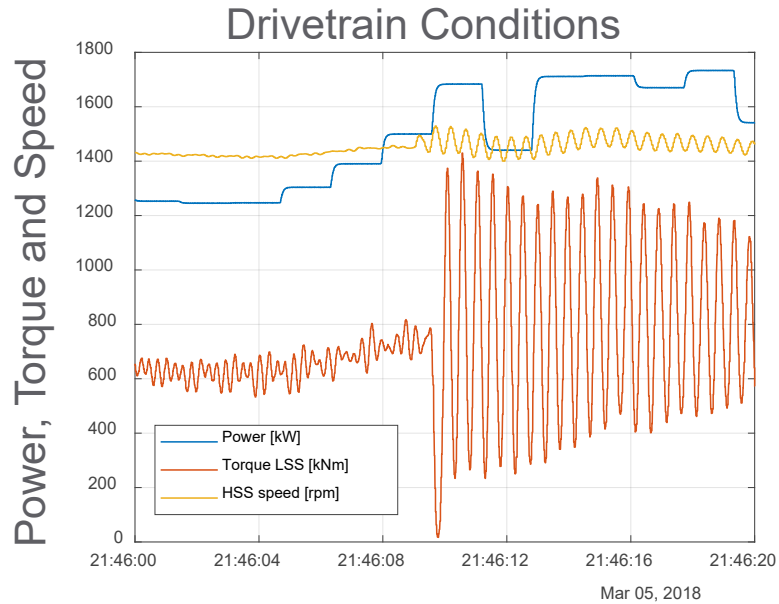


Generator Side

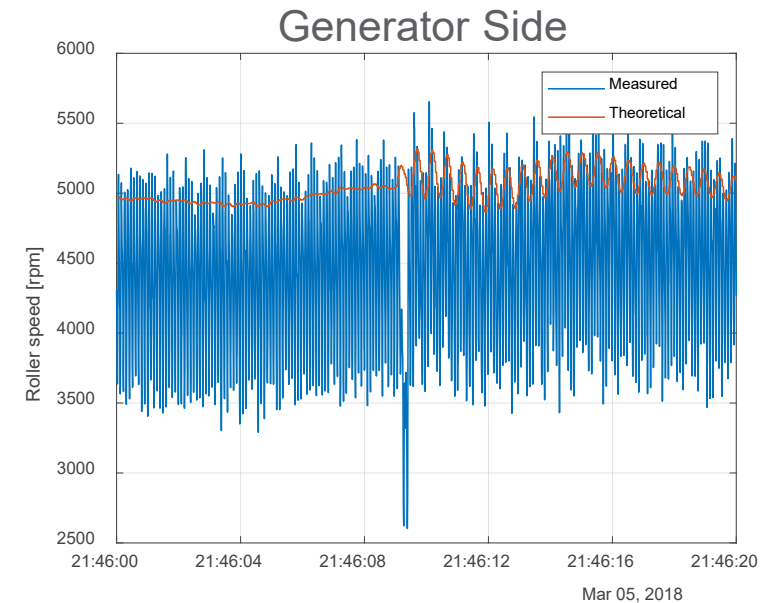
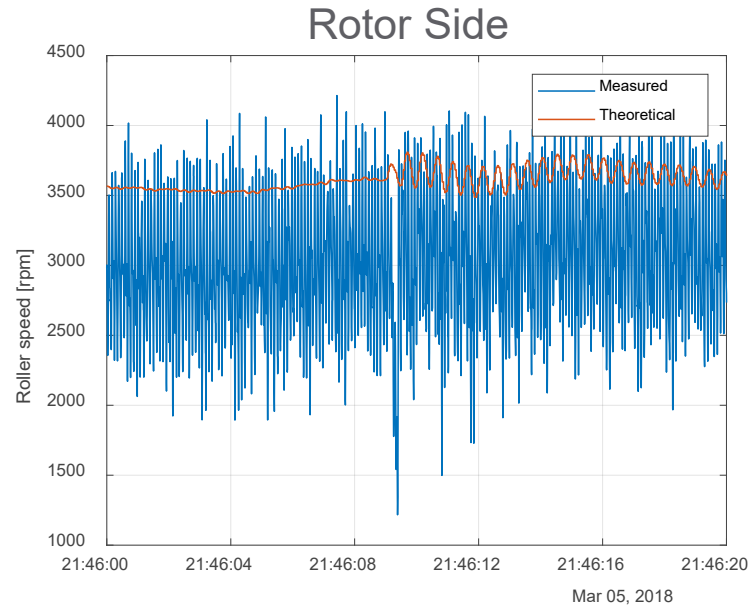


- Torque oscillations at drivetrain 1st eigenfrequency
- Oscillations result in cage and roller dynamics
- Rotor side more sensitive to torque oscillations than generator side
- Roller speed measurements unreliable at low speed conditions.
- At brake engagement roller speed reduces to about 80% slip and accelerates back in about 1.5 seconds.

Transient Conditions – LVRT (50% Drop for 300 milliseconds)

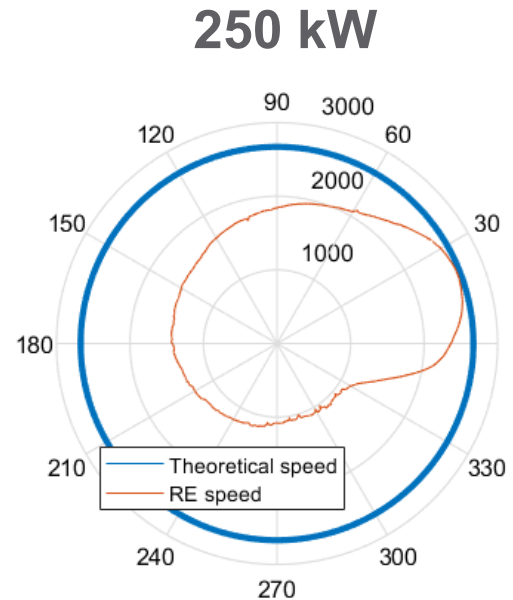
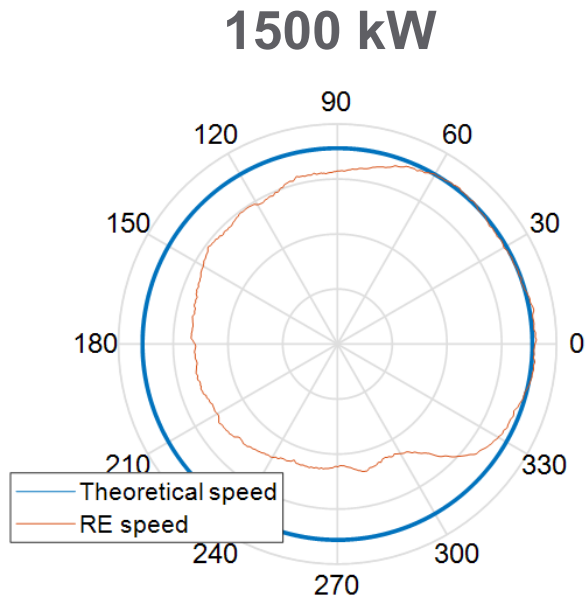


- Torque oscillations at drivetrain 1st eigenfrequency after Low-Voltage Ride Through (LVRT)
- Load oscillations resulting in cage and roller dynamics
- Roller speed reduces to about 50% slip and accelerates back in about 0.5 seconds.

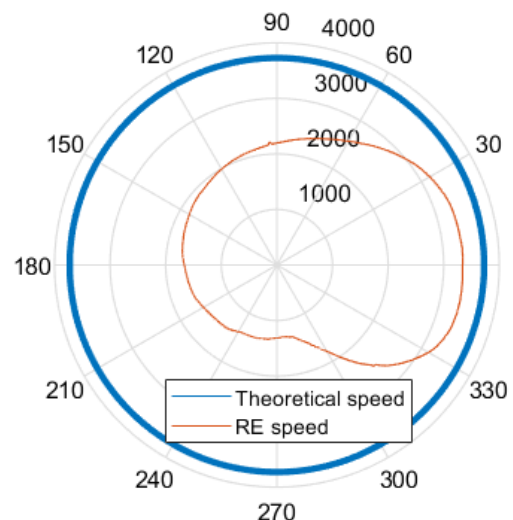
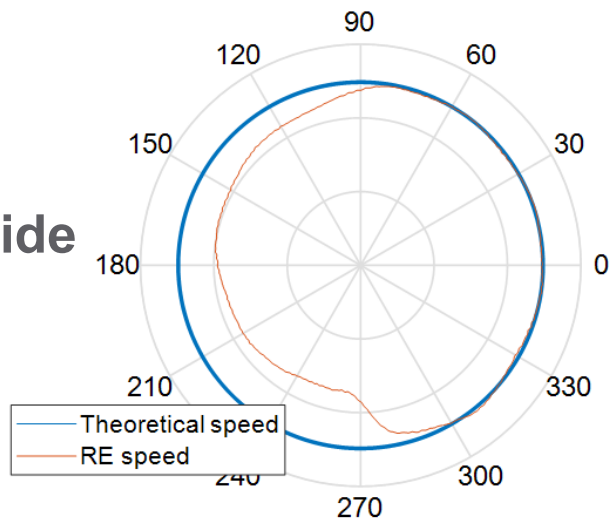


Roller Speed at “Curtailment”

Rotor Side



Generator Side
Inboard



- Operating at low load results in much higher slip levels.

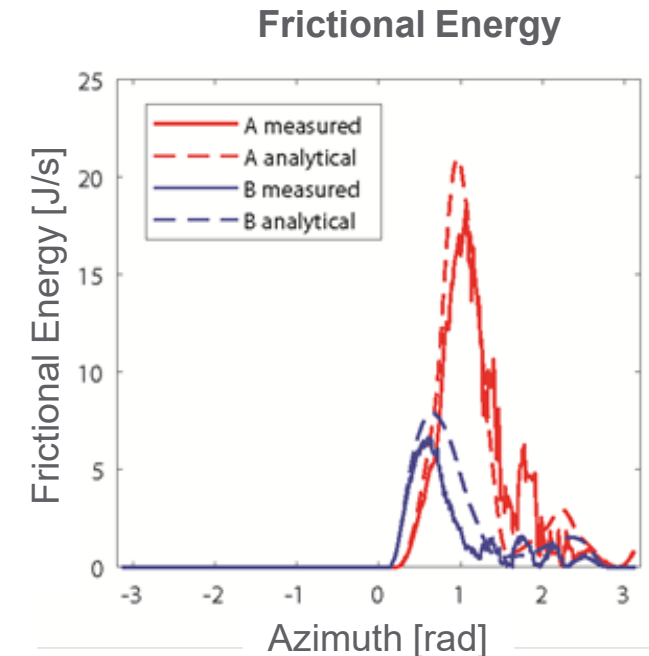
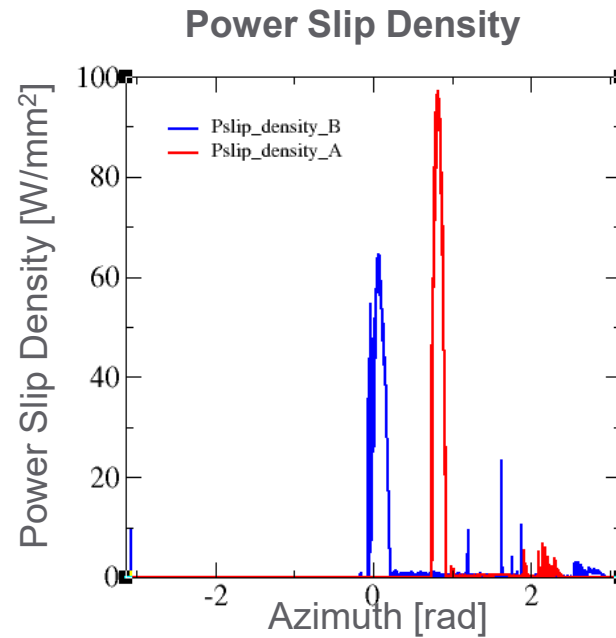
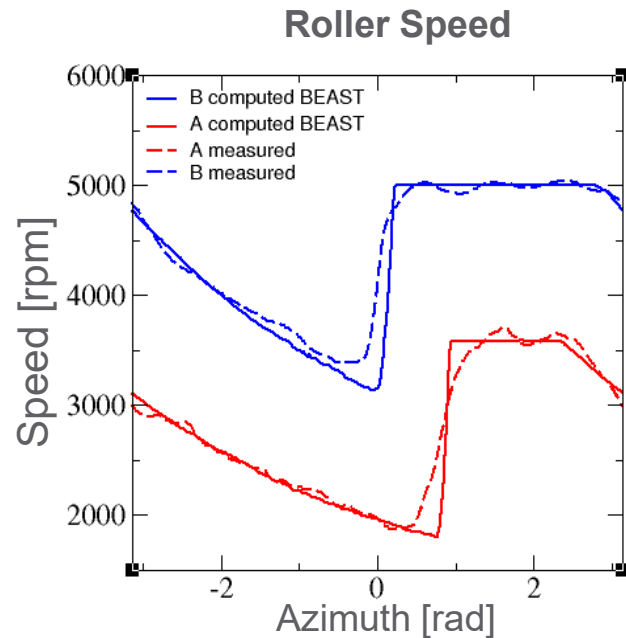
Future Steps and Conclusions



Photo by Dennis Schroeder, NREL 49418

Ongoing Steps

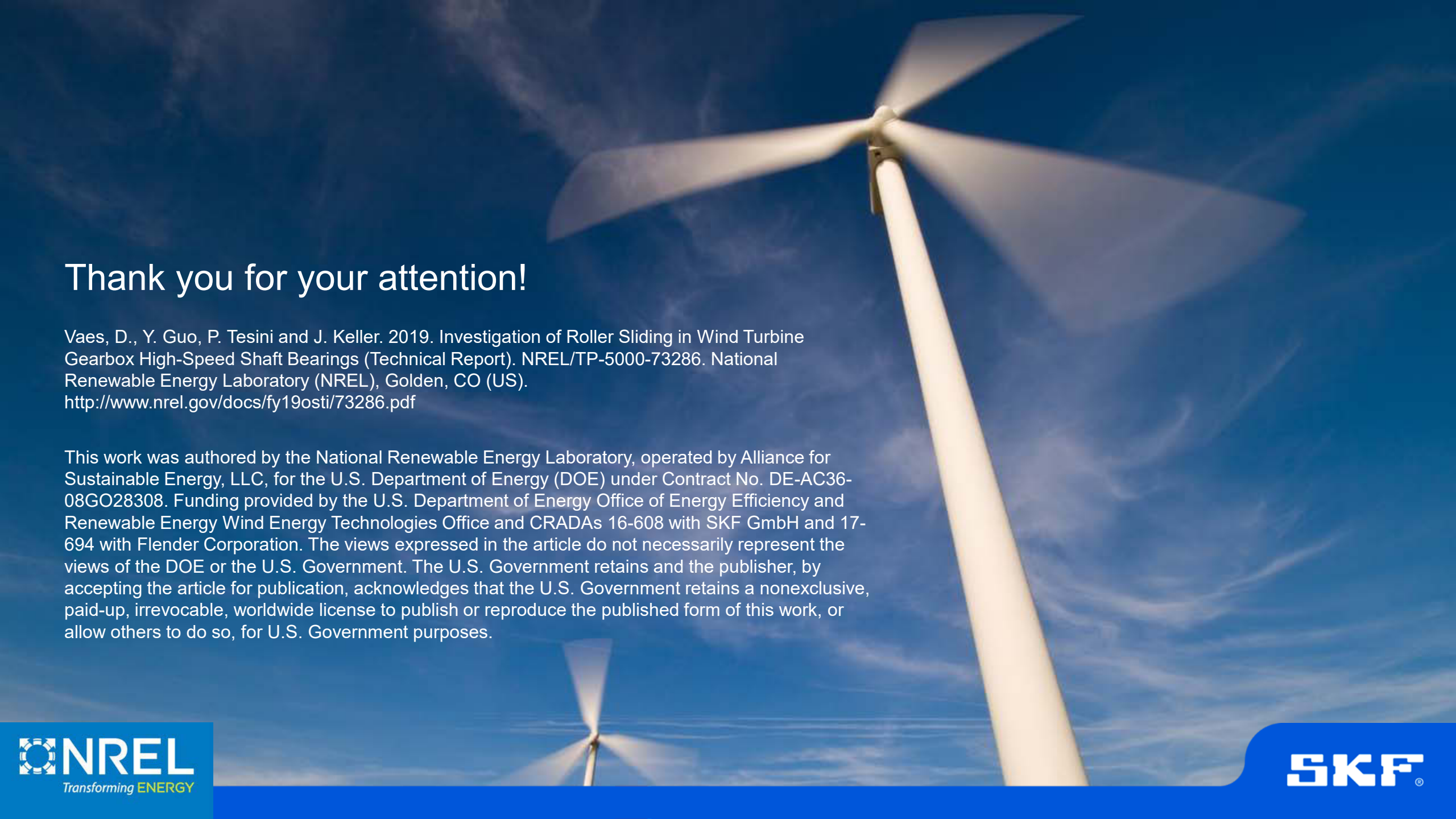
- Repeat the procedure for the cage speed at low load. The proximity sensor is not affected by the same disturbance as the induction coil.
- Simulation of transient conditions (i.e., when measurement cannot be efficiently filtered from noise).
- Use simulation results to evaluate critical conditions for the bearings (e.g., by power slip density or cumulative frictional energy).



W/mm² = watts per millimeters squared | J/s = joules per second

Conclusions

- Measurement of roller and cage speed gives useful insight in the bearing kinematics at different operating conditions:
 - Low load/curtailment
 - Emergency stop
 - LVRT
- High roller slip and accelerations have been measured at these events
- BEAST model has been built and shown to be able to accurately predict roller and cage behaviour at different loads and temperature
- Next steps:
 - Apply and validate the models at special events
 - Evaluate the roller slip losses at special events.



Thank you for your attention!

Vaes, D., Y. Guo, P. Tesini and J. Keller. 2019. Investigation of Roller Sliding in Wind Turbine Gearbox High-Speed Shaft Bearings (Technical Report). NREL/TP-5000-73286. National Renewable Energy Laboratory (NREL), Golden, CO (US).
<http://www.nrel.gov/docs/fy19osti/73286.pdf>

This work was authored by the National Renewable Energy Laboratory, operated by Alliance for Sustainable Energy, LLC, for the U.S. Department of Energy (DOE) under Contract No. DE-AC36-08GO28308. Funding provided by the U.S. Department of Energy Office of Energy Efficiency and Renewable Energy Wind Energy Technologies Office and CRADAs 16-608 with SKF GmbH and 17-694 with Flender Corporation. The views expressed in the article do not necessarily represent the views of the DOE or the U.S. Government. The U.S. Government retains and the publisher, by accepting the article for publication, acknowledges that the U.S. Government retains a nonexclusive, paid-up, irrevocable, worldwide license to publish or reproduce the published form of this work, or allow others to do so, for U.S. Government purposes.